

Copolymerization of propene and 1-hexene with isospecific and syndiospecific metallocene catalysts

Il Kim*, Young Jae Kim

Department of Chemical Engineering, University of Ulsan, P.O. Box 18, Ulsan 680-749, Korea

Received: 16 December 1997/Revised version: 9 February 1998/Accepted: 19 February 1998

SUMMARY

Copolymerization of propene and 1-hexene has been carried out in toluene at 30 °C in the presence of homogeneous methylaluminumoxane (MAO)-activated 3 *ansa*-metallocenes, highly syndiospecific *i*Pr(Cp)(Flu)ZrMe₂ (**1**), lower syndiospecific Et(Cp)(Flu)ZrMe₂ (**2**), and isospecific *rac*-(EBTHI)ZrMe₂ (**3**), in order to study the role of catalyst stereospecificity on comonomer incorporation. The incorporation of 1-hexene decreases in the following order: highly syndiospecific **1**/MAO catalyst > lower syndiospecific **2**/MAO catalyst > isospecific **3**/MAO catalyst. All copolymer chains contain the comonomer in nearly random distribution. The copolymers produced by **1**/MAO and **3**/MAO catalysts were composed of uniform chains, but that by **2**/MAO was fractionated into many fractions in the solvent extraction. Considerable rate enhancements were recorded in the copolymerization when the feed ratio of 1-hexene to propene is around 0.6 for all catalysts.

INTRODUCTION

It has been proposed for the heterogeneous Ziegler-Natta catalysts that catalytic sites having different stereospecificity can show different reactivity toward the comonomer.¹⁾ It has been observed in ethylene/propene copolymerization by homogeneous metallocene catalysts that the reactivity of ethylene varies greatly upon changing the catalyst symmetry (and thus stereospecificity) and that $r_1 \times r_2$ also depends on catalyst structure.²⁾ While values of $r_1 \times r_2 > 1$ are typical of copolymers made with heterogeneous catalysts, values of $r_1 \times r_2 \approx 1$ are observed for copolymers made with metallocene catalysts.^{1,2,3)} Homogeneous metallocene catalysts are known to provide copolymers with narrow composition distribution,²⁾ and this implies that the active site is uniform.³⁾ Therefore, it is possible to synthesize propene random copolymers with new features with respect to those obtained with heterogeneous Ziegler-Natta catalysts. Poly(propene-*co*-ethylene) and poly(propene-*co*-1-butene) copolymers having very low xylene solubles can be obtained by using isospecific metallocenes.⁴⁾ Also, syndiospecific metallocenes have been used to synthesize poly(propene-*co*-1-butene) copolymers having the similar characteristics.⁵⁾

Few data are available for copolymerization with higher α -olefins. In propene/1-hexene copolymerization with metallocene catalysts having different stereospecificity, Soga et al.⁶⁾ found that comonomer reactivity was changed according to the catalyst specificity. The incorporation rate of 1-hexene increases in the following order: aspecific < isospecific < syndiospecific catalyst. A noticeable enhancement of copolymerization activity was observed by increasing MAO/*rac*-(EBI)ZrCl₂ ratio as well as upon mixing MAO and Al(*i*Bu)₃.⁷⁾

The present study describes the effect of metallocene stereospecificity on propene/1-hexene copolymerization with three metallocenes—two syndiospecific catalyst isopropylidene-(cyclopentadienyl-fluorenyl)ZrMe₂ (*i*Pr(Cp)(Flu)ZrMe₂, **1**) and [1,2-(cyclopentadienyl-fluo-

* Corresponding author
e-mail: ilkim@uou.ulsan.ac.kr

renyl)ethane]ZrMe₂ (Et(Cp)(Flu)ZrMe₂, **2**), and an isospecific catalyst *rac*-1,2-ethylene-bis(tetra-hydroindenyl)ZrMe₂ ((EBTHI)ZrMe₂, **3**). Besides the effect on copolymerization activity and molecular weight, the effect on copolymer microstructure is also focused upon.

EXPERIMENTAL

Material Polymerization grade of propene (Korea Petrochemical Co.) was purified by passing it through columns of Fisher RIDOX catalyst and molecular sieve 5A/13X. MAO (8.4 wt% total Al solution in toluene) was purchased from Akzo Chemical. Solvents were distilled from Na/benzophenone and stored over molecular sieves (4 Å). *Ansa*-zirconocene complexes, **1**,⁸⁾ **2**,⁹⁾ and **3**,¹⁰⁾ were synthesized according to previous procedures.

Copolymerization procedure Copolymerization was carried out at 30 °C in a 250 mL glass reactor equipped with a magnetic stirrer. The reactor was filled with 100 mL of toluene, 1-hexene and MAO in a glove box. Then, the reactor was saturated with propene and thermostated. Injecting a prescribed amount of metallocene dissolved in toluene started the polymerization. To keep the molar ratio of 1-hexene ([H]) to propene ([P]) constant, the polymerization was terminated after 10 min or 20 min of reaction by adding a dilute hydrochloric acid solution in ethanol. Polymerization rate was determined at every 0.01 s from the rate of propene consumption, measured by a hot-wire flowmeter (model 5850 D from Brooks Instrument Div.) connected to a personal computer through an A/D converter. The copolymer obtained was filtered, washed with ethanol and dried in vacuum at 40 °C.

Copolymer characterization The ¹³C NMR spectra of copolymers were recorded at 120 °C on a Varian Unity Plus 300 spectrometer operating at 75.5 MHz. Samples for ¹³C NMR spectra were prepared by dissolving 50 mg of polymer in 0.5 mL of C₆D₆/1,2,4-trichlorobenzene (1/5). Melting curves were recorded with a DuPont differential scanning calorimeter (DSC, Model 910) at a 20 °C/min rate. The results of the second scan are reported to eliminate differences in sample history. The intrinsic viscosity of polymers was determined in decalin at 135 °C using an Ubbelohde viscometer. Fractionation of polymer was carried out by using boiling ether, hexane, and heptane for 16 h with a Soxhlet extractor.

RESULTS AND DISCUSSION

Homo- and copolymerization of propene and 1-hexene have been carried out at 30 °C in the presence of 3 metallocene catalysts. Figure 1, 2, and 3 show the polymerization rates as a function of time obtained by using **1**/MAO, **2**/MAO, and **3**/MAO systems, respectively. Figure 4 shows the variation of maximum polymerization rate ($R_{p,max}$) according to [H]/[P] in the feed. Compound **1** bears close resemblance to **2** and behaves accordingly by polymerizing propene to syndiotactic polypropylene (sPP) after activation. However, the sPP by **2**/MAO catalyst produces have higher molecular weight, $\overline{M}_w = 85,000$ (**2**) vs. 73000 (**1**), and broader polydispersity, $\overline{M}_w/\overline{M}_n = 3.2$ (**2**) vs. 1.8 (**1**), though with much lower syndiotacticity, $[rrrr] = 85\%$ vs. 53%. It is interesting to note that **2**/MAO catalyst shows higher catalytic activity than **1**/MAO catalyst by about 2 times in the homopolymerization of propene at similar reaction conditions (Fig. 1(a) and 2(a)). Detailed kinetic behaviors of the two catalytic systems are to be published elsewhere.¹¹⁾

It is not clear why a simple alteration of the bridge, replacement of isopropylidene group by an ethyl group, brings about big difference in catalytic activity. It is possible that both steric and electronic factors are involved but the subject deserves a more in-depth investigation before any statement can be made. Since compound **2** has two carbon atoms in the bridge, the cyclopentadienyl and fluorenyl moieties are pushed further away, adopt a more parallel position. As a result centroid-Zr-centroid angle is increased. According to the X-

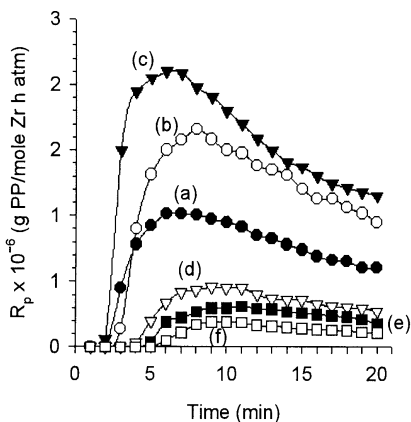


Fig. 1. R_p versus time curve obtained by **1**/MAO catalyst. Polymerization conditions: $T = 30\text{ }^\circ\text{C}$, $P_{\text{C}_3\text{H}_6} = 5\text{ psig}$, $[\text{Al}]/[\text{Zr}] = 1771$, $[\text{Zr}] = 80.3\text{ }\mu\text{M}$, and (a) $[\text{H}]/[\text{P}] = 0$, (b) 0.3, (c) 0.6, (d) 0.9, (e) 1.2, and (f) 1.5.

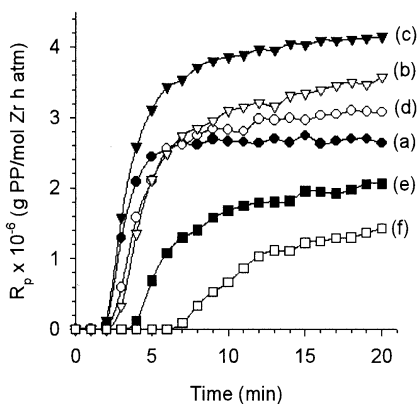


Fig. 2. R_p versus time curve obtained by **2**/MAO catalyst. Polymerization conditions: $T = 30\text{ }^\circ\text{C}$, $P_{\text{C}_3\text{H}_6} = 5\text{ psig}$, $[\text{Al}]/[\text{Zr}] = 2137$, $[\text{Zr}] = 65.7\text{ }\mu\text{M}$, and (a) $[\text{H}]/[\text{P}] = 0$, (b) 0.3, (c) 0.6, (d) 1.2, (e) 1.8, and (f) 2.9.

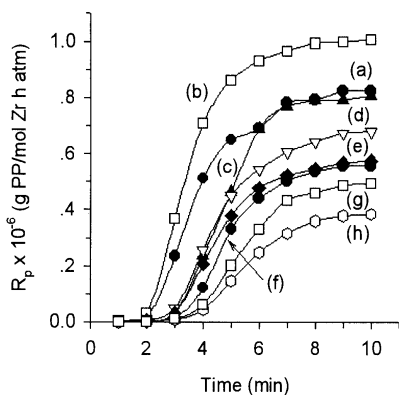


Fig. 3. R_p versus time curve obtained by **3**/MAO catalyst. Polymerization conditions: $T = 30\text{ }^\circ\text{C}$, $P_{\text{C}_3\text{H}_6} = 5\text{ psig}$, $[\text{Al}]/[\text{Zr}] = 1437$, $[\text{Zr}] = 122.0\text{ }\mu\text{M}$, and (a) $[\text{H}]/[\text{P}] = 0$, (b) 0.6, (c) 1.2, (d) 1.8, (e) 2.4, (f) 2.9, (g) 3.5, and (h) 4.1.

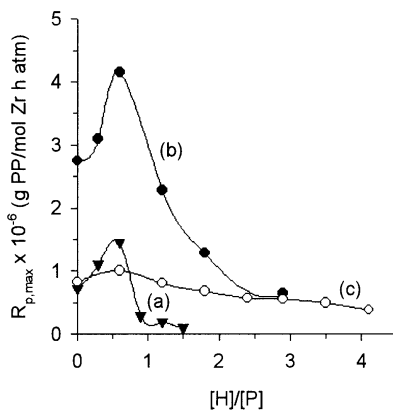


Fig. 4. $R_{p,\text{max}}$ versus $[\text{H}]/[\text{P}]$ ratio obtained by (a) **1**/MAO, (b) **2**/MAO, and (c) **3**/MAO. Polymerization conditions are the same as those in Fig. 1, Fig. 2, and Fig. 3.

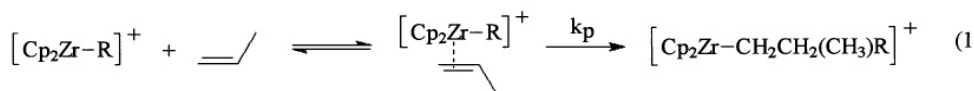
ray diffraction study,⁹ the crystal structure of *pseudo* C_s symmetric $\text{Et}(\text{Cp})(\text{Flu})\text{ZrCl}_2$ exists two types of molecules, two conformers (δ - and λ -conformer). The interatomic bond angles and distances of these conformers are different enough to be considered as two structurally different molecules.⁹ Two conformers interconvert fast enough to be indistinguishable in the NMR time scale.⁹ However, the mobility of their cationic active species activated by excess amount of MAO should be restricted due to contact ion pairing between zirconium alkyl cations and MAO anions. Different from $\text{Et}(\text{Cp})(\text{Flu})\text{ZrCl}_2$, neutral $i\text{Pr}(\text{Cp})(\text{Flu})\text{ZrCl}_2$ is characterized by the prochirality and bilateral symmetry (exact C_s symmetry), and its cationic active species have *S,R*-enantiomeric nature.¹² The difference in the catalytic activity is seemed to be deeply related with these structural differences of the cationic species, especially in solution. These structural differences of the cationic species also influence on the resulting polymer structure. Since **2**/MAO catalyst resembles very much a multi-site system due to an existence of two isomers other than **1**/MAO, **2**/MAO catalyst produces *s*PP having broader polydispersity ($\overline{M}_w/\overline{M}_n = 3.2$) and lower stereoregularity ($[rrrr] = 53\%$) than **1**/MAO.

The propene homopolymerization by **1**/MAO shows decay-rate type profile, on the other hand those by **2**/MAO and **3**/MAO show constant-rate type profile. The maximum rate ($R_{p,\text{max}}$) for the homopolymerization of propene ($[\text{H}]/[\text{P}] = 0$) is in the order of **2**/MAO \gg **1**/MAO \approx **3**/MAO within our experimental range as shown in Fig. 4. The molecular weight of *i*PP produced by **3**/MAO was very low ($\overline{M}_w = 8500$) and $\overline{M}_w/\overline{M}_n$ of the polymer was 1.9. The $[mmmm]$ value of *i*PP obtained by **3**/MAO catalyst was 81 %.

In propene copolymerizations by **1**/MAO (Fig. 1), the rates reach maximum within 10 min, and then decays slowly. As the $[\text{H}]/[\text{P}]$ ratio in the polymerization medium increases, the induction period that shows no activity and the time to reach maximum rate becomes increased. It is interesting to note that considerable enhancement of activity is observed when small amount of 1-hexene is added ($[\text{H}]/[\text{P}]$ ratio < 0.6). At $[\text{H}]/[\text{P}]$ ratio = 0.6, $R_{p,\text{max}}$ is enhanced by two times as shown in Fig. 4. Similar rate acceleration effects on polymerization rate are also observed in **2**/MAO catalyst (Fig. 2). The enhancement of activity is not so large in case of **3**/MAO catalyst.

The activity increase due to the introduction of a small amount of comonomer (the so called "second monomer effect") also detected by many authors in the copolymerization of ethylene/higher α -olefins,^{13,14} propene/1-octene,¹⁵ and propene/1-hexene⁷ by using various metallocene catalysts. The simplest and most likely explanation to explain it is that the lower crystallinity and/or the higher solubility of a copolymer in the polymerization medium might allow for higher rates of diffusion of the monomers to the catalyst center. The enhancement of activity may also emerge from the growing number of active centers due to the addition of α -olefin. This is probably so because the centers were not all active for the homopolymerization. Another possible explanation is that the rate constant of propagation raises by the addition of comonomer.

In all copolymerizations (Fig. 1, 2, and 3), the induction period, in which no absorption of propene is observed, increases as $[\text{H}]/[\text{P}]$ ratio in monomer feed increases. According to the proposed mechanisms,^{16,17} the olefin monomer binds to the cationic metallocene-alkyl complex to give an alkyl olefin intermediate and then is inserted between the metal the alkyl group to give the growing polymer:



The induction period found in the copolymerization can be induced by the delayed migratory insertion of propene (second step of Reaction (1)) due to the presence of 1-hexene. However, this is true only at the initial stage of polymerization when R is small, because there is no significant difference between relative reactivity of propene and 1-hexene ($r_H \times r_P \approx 1$) (*vide infra*) and the polymerization rate increases to $R_{p,max}$ very fast right after induction period.

The copolymers have been characterized by various methods and the results are summarized in Table 1. The monomer reactivity ratios r_P and r_H (P = propene, H = 1-hexene) were estimated from the ^{13}C NMR spectra using the following equations:

$$r_P = 2 [\text{PP}]/([\text{PH}] X) \text{ and } r_H = 2 [\text{HH}]/([\text{PH}] X)$$

where $[\text{PP}]$, $[\text{PH}]$ and $[\text{HH}]$ denote dyad sequence distributions in the copolymers, and X is the concentration ratio of propene to 1-hexene in the feed, $[\text{P}]/[\text{H}]$.

The melting point (T_m) of sPP produced by 1/MAO was 133 °C, but sPP by 2/MAO had no melting peak in DSC analysis. The two sPPs obtained by 1/MAO and 2/MAO catalyst were also characterized by fairly different T_g values, 2.2 °C and -15.3 °C, respectively. All copolymers obtained by these catalysts had no T_m . The T_g values of copolymers decreased as the amount of 1-hexene incorporated in copolymer increases. The melting point of *i*PP obtained by 3/MAO catalyst was 132.3 °C. The T_m values of copolymers decreased sharply to 52.4 °C when $[\text{H}]$ in copolymer is 19.2 %. Any further increase of $[\text{H}]$ resulted in disappearing of T_m . The T_g values of copolymers produced by 3/MAO were lower than those obtained by 1/MAO or 2/MAO.

The molecular weights of copolymers obtained by syndiospecific catalysts could be assumed to be similar, but higher than those obtained by isospecific catalyst by about 10 times. For all catalytic systems, the molecular weight did not change so much according to the amount of 1-hexene incorporated in copolymer; on the contrary it changes slightly in line with the rate of polymerization.

From the plot of $[\text{H}]$ in copolymer vs. $[\text{H}]$ in feed (Fig. 5) and the monomer reactivity ratios summarized in Table 1, it can be said that the reactivity of 1-hexene is in the order of 1/MAO > 2/MAO > 3/MAO. This result indicates that syndiospecific catalysts show higher reactivity toward 1-hexene than isospecific catalyst. Similar results have been reported by Soga, et al.⁶⁾ Considering that there is a large difference in syndiospecificity between 1/MAO and 2/MAO, the higher reactivity toward 1-hexene is achieved with higher syndiospecific catalyst. And it can also be confirmed by comparing with the reference data⁶⁾ that there is no difference of comonomer reactivity between *i*-Pr(Cp)(Flu)ZrMe₂/MAO and *i*-Pr(Cp)(Flu)ZrCl₂/MAO catalysts. The product of monomer reactivity ratios ($r_P \times r_H$) which can be utilized to speculate the copolymer structure are all in a similar range, 0.64 - 1.71, regardless of the catalytic systems as shown in Table 1. This range of value demonstrates that all copolymers investigated in this study have a nearly random sequence distribution. Thus, all stereospecific catalysts of this study appear to follow Bernoullian propagation statistics.

Solvent fractionation of polymers by using boiling ether, hexane, and heptane shows that sPP produced by 1/MAO and *i*PP by 3/MAO have similar solubility in that they are mostly soluble in heptane (Table 1). However, sPP obtained by 3/MAO is evenly soluble in all solvents and 21.1 % of it is insoluble to even heptane. The fractionation behavior demonstrates that 1/MAO and 3/MAO catalysts form uniform active species but 2/MAO catalyst forms multiple active species. The similar fractionation behavior has been observed in copolymers; the copolymers produced by 1/MAO and 3/MAO catalysts are mostly soluble

Table 1. Results of propene/1-hexene copolymerization with various stereospecific catalysts.^{a)}

| Run No. | Compd. | [H] in feed (mol-%) | [H] in copolymer (mol-%) | R _{p,max} (kg PP/mol Zr h atm) | [PH] (%) | [HH] (%) | r _P ^{b)} | r _H ^{b)} | r _P × r _H | T _g ^{c)} (°C) | $\overline{M}_n^{d)}$ × 10 ⁻⁴ (g/mole) | Ether sol. (wt %) | Hexane sol. (wt %) | Heptane sol. (wt %) | |
|-----------|----------|---------------------|--------------------------|---|----------|----------|------------------------------|------------------------------|---------------------------------|-----------------------------------|---|-------------------|--------------------|---------------------|-----|
| Fig. 1(a) | 1 | 0.0 | 0.0 | 1015 | 100.0 | 0.0 | - | - | - | 2.2 | 6.1 | 0.0 | 9.1 | 90.9 | |
| Fig. 1(b) | | 22.7 | 10.0 | 1657 | 80.0 | 0.0 | 2.35 | - | - | -4.6 | 7.1 | - | - | - | |
| Fig. 1(c) | | 37.0 | 14.5 | 2065 | 73.6 | 23.8 | 2.6 | 3.64 | 0.37 | 1.35 | -6.9 | 6.2 | 12.6 | 79.9 | 7.5 |
| Fig. 1(d) | | 46.9 | 22.5 | 456 | 60.0 | 36.5 | 3.5 | 2.90 | 0.22 | 0.64 | -9.0 | 5.4 | - | - | - |
| Fig. 1(e) | | 54.1 | 29.5 | 310 | 51.0 | 39.0 | 10.0 | 3.08 | 0.44 | 1.36 | -9.5 | 5.1 | - | - | - |
| Fig. 1(f) | | 59.5 | 42.5 | 191 | 34.0 | 47.0 | 19.0 | 2.12 | 0.55 | 1.17 | -15.7 | 4.8 | - | - | - |
| Fig. 2(a) | 2 | 0.0 | 0.0 | 2750 | 100.0 | 0.0 | - | - | - | -15.3 | 7.2 | 14.5 | 35.4 | 29.0 ^{e)} | |
| Fig. 2(b) | | 22.7 | 10.5 | 3107 | 79.0 | 21.0 | 0.0 | 2.21 | - | -4.1 | 6.8 | - | - | - | |
| Fig. 2(c) | | 37.0 | 13.4 | 4151 | 73.3 | 26.7 | 0.0 | 3.22 | - | -5.9 | 6.4 | 37.8 | 42.1 | 18.2 ^{f)} | |
| Fig. 2(d) | | 54.1 | 21.4 | 3584 | 63.0 | 33.3 | 4.7 | 4.46 | 0.24 | 1.07 | -10.3 | 5.8 | - | - | |
| Fig. 2(e) | | 63.8 | 39.6 | 2062 | 37.5 | 45.8 | 16.7 | 2.89 | 0.41 | 1.18 | -15.2 | 4.9 | - | - | |
| Fig. 2(f) | | 74.6 | 56.5 | 1427 | 19.5 | 48.0 | 32.5 | 2.39 | 0.46 | 1.10 | -19.5 | - | - | - | |
| Fig. 3(a) | 3 | 0.0 | 0.0 | 825 | 100.0 | 0.0 | 0.0 | - | - | 16.6 | 0.79 | 0.0 | 15.7 | 84.3 | |
| Fig. 3(b) | | 37.0 | 9.4 | 1008 | 82.0 | 17.1 | 0.9 | 5.63 | 0.18 | 1.01 | -21.0 | 0.63 | 74.2 | 25.8 | 0.0 |
| Fig. 3(c) | | 54.1 | 19.2 | 808 | 66.5 | 28.6 | 4.9 | 5.48 | 0.29 | 1.59 | -26.1 | 0.54 | - | - | - |
| Fig. 3(d) | | 63.8 | 24.4 | 679 | 58.2 | 34.8 | 7.0 | 5.90 | 0.23 | 1.36 | -29.3 | 0.48 | - | - | - |
| Fig. 3(e) | | 70.2 | 30.8 | 575 | 50.3 | 37.9 | 11.8 | 6.25 | 0.26 | 1.63 | -27.7 | 0.41 | - | - | - |
| Fig. 3(f) | | 74.6 | 37.3 | 554 | 40.9 | 43.7 | 15.4 | 5.50 | 0.24 | 1.32 | -30.0 | 0.37 | - | - | - |
| Fig. 3(g) | 77.9 | 40.0 | 494 | 39.1 | 41.9 | 19.0 | 6.58 | 0.26 | 1.71 | -33.7 | 0.40 | - | - | - | |
| Fig. 3(h) | 80.5 | 43.8 | 383 | 33.6 | 45.3 | 21.1 | 6.12 | 0.23 | 1.41 | -37.5 | 0.34 | - | - | - | |

^{a)}Polymerization conditions are indicated in corresponding Figures in Run No. ^{b)}r_P, r_H: Reactivity ratios of propene and 1-hexene, respectively. ^{c)}T_g = Glass transition temperature measured by DSC. ^{d)}M_n = Viscosity-average molecular weight. ^{e)}Remained fraction after heptane fractionation is 21.1 wt %. ^{f)}Remained fraction after heptane fractionation is 1.9 wt %.

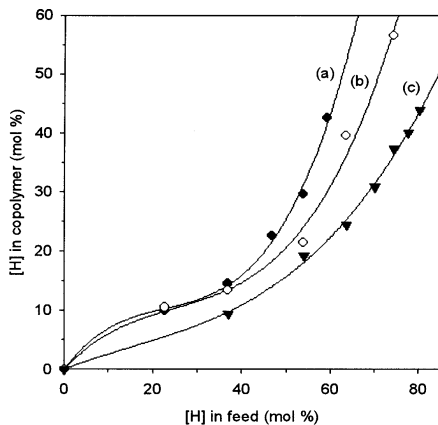


Fig. 5. Percentage of comonomer incorporated in the copolymer against comonomer content in the feed for propene/1-hexene copolymerizations with (a) **1**/MAO catalyst, (b) **2**/MAO catalyst, and (c) **3**/MAO catalyst.

in ether and hexane, but the copolymer by **2**/MAO is fractionated into many fractions.

The authors wish to acknowledge the financial support of the Korea Research Foundation made in the program year of 1997..

REFERENCES

- Cheng HN, Kakugo M (1991) *Macromolecules* 24: 1724
- Zambelli A, Grassi A, Galimberti M, Mazzocchi R, Piemontesi F (1991) *Makromol Chem Rapid Commun* 12: 523.
- Kaminsky W, Miri M (1985) *J Polym Sci Polym Chem Ed* 23: 2151.
- European Patent Appl. 318049 (1988) Ausimont S.r.l.
- European Patent Appl. 464684 (1991) HIMONT Incorporated.
- Uozumi T, Soga K (1992) *Makromol Chem* 193: 823.
- Forlini F, Tritto I, Locatelli P, Sacchi, MC (1997), *Macromol Chem Phys* 198: 2397.
- Ewen JA, Jones RL, Razavi A, Ferraa JD (1988) *J Am Chem Soc* 110: 6255.
- (a) Patsidis K, Palackal SJ, Alt HG, European Patent Appl. 512554 A2 (1992); (b) Razavi A, Vereecke D, Peters L, Hessche DV, Den Dauw K, Nafpliotis L, de Froimont Y (1993) *SPO* 1993, 105; (c) Razavi A, Peters L, Nafpliotis L, Atwood JL (1994) in *Studies in Surface Science and Catalysis, Proceedings of the International Symposium on Catalyst Design for Tailor-made Polyolefins*, Soga K, Terano M, eds, Kodansha, Tokyo, p 411; (d) Razavi A, Peters L, Nafpliotis L (1997) *J Mol Cat A: chemical*, 115: 129.
- Kaminsky W, Kulper K, Brintzinger HH, Wild FRWP (1985) *Angew Chem* 97: 507.
- Kim I, Kim KT (1997) *J Appl Polym Sci* revised for publication.
- (a) Ewen JA (1984) *J Am Chem Soc* 106: 6355; (b) Ewen JA, Elder MJ (1993) *Makromol Chem Macromol Symp* 66: 179.
- Herfert H, Montag P, Fink G (1993) *Makromol Chem* 194: 3167.
- Quijada R, Dupont J, Miranda MSL, Scipioni RB, Galland GB (1995) *Macromol Chem Phys* 196: 3991.
- Jungling S, Koltzenburg S, Mulhaupt R (1997) *J Polym Sci A* 35:1.
- Cossee P (1964) *J Catal* 3:80.
- Ivin K, Rooney J, Stewart C, Green M, Mahtab R (1978) *J Chem Soc Chem Commun* 604.